

Design of a new ultra-small polarization converter in InGaAsP/InP membrane

J. Pello, J.J.G.M. van der Tol, G. Roelkens, H.P.M.M. Ambrosius and M.K. Smit
COBRA Research Institute, Eindhoven University of Technology (TUE)
Eindhoven, The Netherlands
j.pello@tue.nl

Abstract—The design of an ultra-small (4.1 μm length) polarization converter in Indium phosphide (InP) membrane is presented. The device is modelled using a vectorial 2D mode solver. Simulations show strong conversion ($> 98\%$) and low-loss operation (< 0.6 dB) over a wavelength range of 200 nm. A description of a possible fabrication scheme for the device using standard InP technology is also given.

Indium phosphide; integrated optics; polarization converter (PC); triangular waveguide.

I. INTRODUCTION

Recently, membrane photonics platforms such as Silicon-on-insulator (SOI) or InP-membranes-on-silicon (IMOS) have been gaining attention. The high vertical index contrast obtainable in membrane structures can lead to high density photonic integrated circuits (PICs) by reducing substantially the size of most photonic devices. Furthermore, membranes are compatible with different carrier substrates through the use of bonding technologies [1], which paves the way for intrachip communication.

Although the SOI platform benefits from the technology tools developed in the silicon industry, it lacks the ability of creating simple optical sources and amplifiers. By contrast, the IMOS platform is based on direct bandgap alloys, and we are working on butt-joint integration of active and passive components in thin InP-membrane, using sub-micron scale selective area growth. Recently, the fabrication of compact and efficient passive IMOS components was presented [2], including ultra-small couplers, ring resonators and micro-bends (see Fig. 1). In the present paper, a new device, an ultra-small polarization converter in InP membrane, is introduced, using two oppositely-oriented triangular waveguide sections.

The presented device is more than one order of magnitude smaller than the shortest polarization converters made by optical lithography [3], and was designed together with a clear fabrication plan which uses the standard technological tools available for InP processing. The polarization conversion behaviour is analyzed using the film mode matching (FMM)

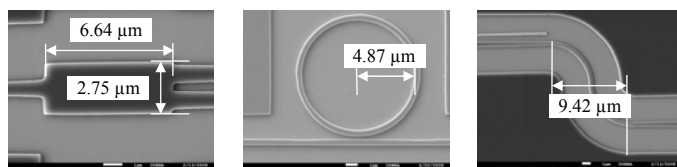


Figure 1. An ultra-small coupler, a ring resonator and an S-bend previously realized in IMOS

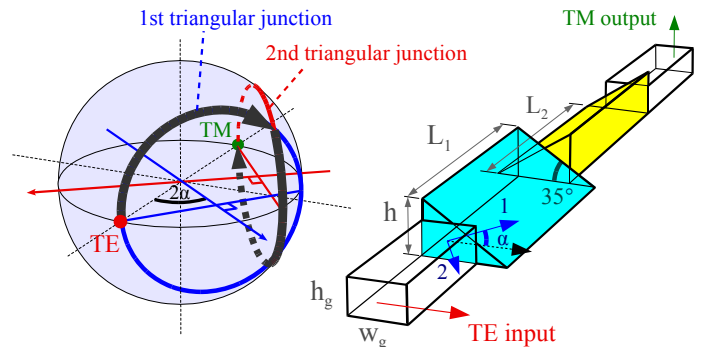


Figure 2. Schematic of the polarization converter design and Poincaré sphere diagram of the polarization conversion

method [4]. This component can be applied to polarization-diversity integration schemes and in interesting devices such as light intensity modulators and polarization bit interleaving (PBI) components [5].

II. PRINCIPLE

The idea behind the use of asymmetrical cross-section waveguides in PCs is to create a new set of two eigenmodes which are not aligned with the TE and TM polarization of the normal rectangular waveguides, and which propagate with different propagation constants β_1 and β_2 . The incoming polarization state, e.g. TE in Fig. 2, is projected on these two tilted eigenmodes. As the eigenmodes propagate with different speeds, a phase-shift is created between the two that linearly increases with the propagation length L (the same birefringence principle as in bulk half-wave plates). By choosing the length L of the triangular section and coupling light back to a rectangular waveguide, different elliptical and linear polarization states can be obtained.

In this work, we consider triangular waveguides that can be obtained by dry etching of the vertical wall and wet etching of the slanted wall at an angle of 35° with respect to the (001) plane [6]. The resulting asymmetry yields a rotation $\alpha \sim 23^\circ$ (determined using the FIMMWAVE mode solver [4]) of the eigenmodes of the triangular waveguides. As a consequence, the polarization states attainable by varying the length of the first triangular waveguide are all the states represented by the first drawn circle on the Poincaré sphere in Fig. 2. We see that in order to achieve full TE to TM conversion, one triangular section is not enough. Therefore, we add another triangular section, mirrored with respect to the first one, which will enable to reach the TM polarization state by rotating along the semi-dotted circle on the sphere in Fig. 2. The two bold arrows

in the sphere show how the polarization is gradually converted from TE to TM.

The respective lengths of the two triangular sections that lead to full TE to TM conversion can be obtained by simple geometric calculations in the Poincaré sphere and expressed in terms of the half-beat length $L_\pi = \frac{\pi}{\beta_1 - \beta_2}$ and the tilt angle α as:

$$L_1 = \frac{L_\pi}{\pi} \times \left(\arcsin\left(\frac{1}{(\tan 2\alpha)^2}\right) + \frac{\pi}{2} \right) = 2L_\pi - L_2 \quad (1)$$

The device has a total length of $2L_\pi$. As expected, the stronger the birefringence of the waveguide, the shorter the device.

III. DESIGN OPTIMIZATION AND TOLERANCES

The structure is modelled in FIMMWAVE, taking into account the Benzocyclobutene (BCB) and air claddings of a fabricated device (see Section IV).

We first investigate the performance of the PC at a wavelength of $\lambda = 1.55 \mu\text{m}$. The propagation constants β_1 and β_2 of the two modes of the triangular waveguides are calculated using the mode solver FIMMWAVE for different values of the membrane height h . It is found that the highest birefringence is obtained for $h = 400 \text{ nm}$. The corresponding half-beat length is equal to $L_\pi = 2.06 \mu\text{m}$, which corresponds to a total device length of only $4.12 \mu\text{m}$. After setting h to this value, the cross-section dimensions h_g and w_g (see Fig. 2) of the input (and output) rectangular waveguides, as well as the lateral offsets between the different junctions are optimized to maximize the coupling efficiency. It is found that the coupling between rectangular and triangular waveguides is optimized for $h_g/h \sim 2/3$. This suggests the use of a very thin etch-stop layer in the membrane to enable a simple and accurate definition of these two heights. A 20 nm-thick quaternary etch-stop layer was therefore included in the simulation of the triangular waveguides.

To verify the behaviour of the complete PC and investigate its tolerance to different fabrication parameters variations, we simulate it in the propagation module of FIMMWAVE. As seen on the results graph in Fig. 3, the short length of this PC makes it very broadband. For the 1.4-1.6 μm wavelength range, the device total losses are less than 0.6 dB and the polarization conversion (defined as the TM output power divided by the total output power for a fully TE polarized input wave) is more than 98%. The use of wet-etching, which enables to set the slope of the slanted wall of the triangular junctions very

accurately to 35° and to define the two heights h and h_g , makes our design intrinsically tolerant. According to our simulations, an error of 20 nm in the definition of the height h of the triangular section (respectively, an error of 100 nm in the rectangular waveguides width) increases the losses by only 0.1 dB without changing the polarization conversion.

IV. FABRICATION PLAN

Like our previous IMOS components [2], the presented polarization converter will first be fabricated on an epitaxial InP and quaternary layer structure. Then, the sample is bonded upside-down with BCB on a host wafer and the substrate and sacrificial layers are removed. In the end, only the submicron-thick patterned InP membrane is left, embedded in BCB and its bottom surface facing the air.

First the heights h and h_g are defined using the quaternary etch-stop layer mentioned in section III. The rectangular waveguides can then be fabricated by standard e-beam lithography and dry-etching as in [2]. For the triangular waveguides, we propose to adapt the process flow successfully applied in classical InP-based waveguides [3]. The vertical sidewalls are defined by dry etching in the same step as the rectangular waveguides. The area of the triangular sections is then covered with a SiN_x mask, which is dry-etched to leave only the vertical sidewalls covered. Successive wet-etchings of InP, using e.g. $1\text{HCl}:1\text{H}_3\text{PO}_4$ [6], and of the thin quaternary etch-stop layer, will stop on the (112) plane between the SiN_x covered wall and the etch-stop layer below, thus defining quasi-perfect triangular cross-section waveguides.

V. CONCLUSION

We present the design of a new IMOS component, used for efficient TE to TM conversion. The device shows excellent broadband capabilities, is inherently tolerant and can be fabricated using standard InP membrane technology. It is one order of magnitude smaller than the shortest PCs made to date by optical lithography. This device can be used with other devices of the IMOS platform to realize high-density and eventually fully active-passive PICs suitable for inter and intrachip communication.

REFERENCES

- [1] G. Roelkens, J. van Campenhout, J. Brouckaert, D van Thourhout, R. Baets, P. Rojo Romeo et al., "III-V/Si photonics by die-to-wafer bonding," *Materials Today*, vol. 10, no. 7-8, Jul. 2007
- [2] F. Bordas, F. van Laere, G. Roelkens, E.J. Geluk, F. Karouta, P.J. van Veldhoven et al. "Compact grating coupled MMI on DVS-BCB bonded InP-membrane," 14th European Conference on Integrated Optics, ECIO08, Eindhoven, 11-13 Jun. 2008
- [3] L.M. Augustin, R. Hanfoug, J.J.G.M. van der Tol, W.J.M. de Laat and M.K. Smit, "A compact integrated polarization splitter/converter in InGaAsP-InP," *IEEE Photon. Technol. Lett.*, vol. 19, no. 17, Sep. 2007
- [4] FIMMWAVE v.5.1, Photon Design, 2008
- [5] P. S. Cho and J. B. Khurgin, "Return-to-zero differential binary phase-shift-keyed multichannel transmission with 25-Gbit/s polarization bit interleaving and 25-GHz spacing," *Journal of optical networking*, vol. 2, no. 5, May 2003
- [6] S. Adachi and H. Kawaguchi "Chemical Etching Characteristics of (001) InP," *J. Electrochem. Soc.*, vol. 128, no. 6, p. 1342, Jun. 1981

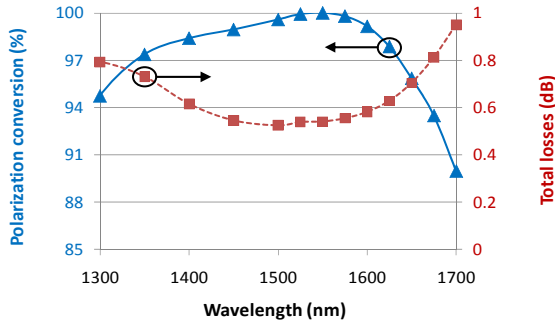


Figure 3. Spectral behaviour of the proposed PC design optimized for $\lambda = 1.55 \mu\text{m}$